

Vacuum ultraviolet spectroscopy of excitons in solid krypton

This article has been downloaded from IOPscience. Please scroll down to see the full text article.

2002 J. Phys.: Condens. Matter 14 5529

(<http://iopscience.iop.org/0953-8984/14/22/306>)

View [the table of contents for this issue](#), or go to the [journal homepage](#) for more

Download details:

IP Address: 171.66.16.104

The article was downloaded on 18/05/2010 at 06:45

Please note that [terms and conditions apply](#).

Vacuum ultraviolet spectroscopy of excitons in solid krypton

Vambola Kisand^{1,3}, Marco Kirm², Sebastian Vielhauer²
and Georg Zimmerer²

¹ Institute of Physics, University of Tartu, Riia 142, 51014 Tartu, Estonia

² Institut für Experimentalphysik, Universität Hamburg, Luruper Chaussee 149,
D-22761 Hamburg, Germany

E-mail: vamps@fi.tartu.ee

Received 5 March 2002

Published 23 May 2002

Online at stacks.iop.org/JPhysCM/14/5529

Abstract

The emission of free and self-trapped excitons in solid Kr was investigated using luminescence spectroscopy in the vacuum ultraviolet region. The influence of the sample crystal structure and Xe impurity on the shape and location of the self-trapped exciton band was observed directly using samples grown under different conditions from gases with various degrees of purity. For the first time, the luminescence spectra were measured for practically Xe-free solid Kr samples of high structural quality.

New high-resolution reflection spectra of solid Kr were measured as well. Due to the good quality of the samples and excellent vacuum conditions, a new member of the exciton series ($n = 5$) was revealed. On the basis of high-resolution reflection measurements, more accurate values of several parameters concerning excitons in solid Kr were determined.

1. Introduction

Solid Kr, like other rare-gas solids (RGSs), is one of the simplest solids. The peculiar properties of RGSs are a consequence of the closed-shell electronic configuration of the atoms (Ne–Xe ns^2np^6 , $n = 2, \dots, 5$). The binding energies of the valence electrons are so large that the closed-shell nature of the atoms is conserved in the condensed phase, in which the atoms are held together by van der Waals forces. As a result of the high ionization energy of atoms, RGSs are dielectrics with extremely large forbidden gaps (for solid Kr $E_g = 11.59$ eV).

Solid Kr is an ideal model substance for investigations of excitonic excitations. Excitonic effects are observable in absorption, reflection and the luminescence spectra of solid Kr [1–3]. While absorption and reflection spectra offer information about electronic excitations at the

³ Author to whom any correspondence should be addressed.

moment of their creation, the luminescence spectra give information about the system after certain relaxation processes. The valence band of solid Kr is split into two sub-bands due to the spin-orbit splitting. Therefore, two exciton series are observable in absorption/reflection spectra. Excitons consisting of an electron bound to the valence hole with total angular momentum $j = \frac{3}{2}$ or $\frac{1}{2}$ are often called $\Gamma(\frac{3}{2})$ or $\Gamma(\frac{1}{2})$ excitons, respectively.

The most interesting aspect of exciton-type luminescence of solid Kr is the coexistence of free excitons (FEs) and self-trapped excitons (STEs) due to the energy barrier separating the respective states. As a result, broad-band STE luminescence as well as narrow-band FE luminescence are simultaneously observable. The strength of the FE emission line strongly depends on the sample quality. In the context of the present paper we mean by 'good-quality' samples polycrystalline samples where the size of the micro-crystallites is significantly larger than the scattering length of the FE on the acoustic phonons. Intense FE emission is observable only in this kind of sample. Additionally, the purity of Kr is very important, since even some tens of ppm Xe in Kr cause strong Xe luminescence, suppressing significantly the FE luminescence of solid Kr. In defect-rich samples (which are referred to as 'snowlike' hereafter), the FEs will be trapped at defects (e.g. grain boundaries, vacancies etc) before they can decay radiatively, and FE emission is not observable. Therefore, the ratio of FE and STE emission band intensities is used as a measure of sample quality [3].

It is important to point out that all members of the excitonic series observable in reflection/absorption spectra are FEs, which can transport energy through the crystal. Nevertheless, in the literature (including the present work), the term 'free exciton' is used very often as a synonym for the first member of the $\Gamma(\frac{3}{2})$ exciton series, since luminescence is observable only from this (lowest excitonic) state.

In the past, studies of solid Kr have been influenced by nearly unavoidable Xe impurities. The aim of the present work was to investigate emission of free and self-trapped excitons in Xe-free solid Kr using luminescence spectroscopy in the vacuum ultraviolet (VUV) region. In particular, we paid attention to the influence of the sample crystal structure and the Xe impurity on the STE band. Additionally, new high-resolution reflection measurements were performed.

2. Experimental details

The experiments were carried out at the experimental station Superlumi located at Hasylab (*Hamburger Synchrotronstrahlungslabor*) at DESY (*Deutsches Elektronen-Synchrotron*) [4]. Selective photon excitation with a resolution interval between $\Delta\lambda = 0.6$ and 3.5 Å was used. Spectral analysis of luminescence was carried out with a high-resolution VUV monochromator in combination with a multichannel plate-type position sensitive detector (resolution $\Delta\lambda = 1.1$ Å). Reflection spectra were measured at an angle of incidence of 17.5° . During measurements, the pressure in the sample chamber was lower than 1×10^{-9} mbar.

The crucial part of the experiments was the sample preparation. Good-quality, visually transparent Kr samples with a thickness of about 0.3 mm were grown from the gas phase (at an average growth rate of $2 \mu\text{m min}^{-1}$) near thermodynamic equilibrium conditions at 84 K. Finally, the crystals were slowly cooled down (about 1 K min^{-1}). As discussed before, by good-quality Kr samples we mean homogeneous samples with very small amounts of impurities and as-grown defects, where the size of the micro-crystallites is significantly larger than the scattering length of the FEs on acoustic phonons. For sample preparation, krypton with the highest commercially available purity (Spectra Gases Inc., 99.999%, Xe < 5.0 ppm) was used.

For comparison, some samples were grown in a different way: Kr gas was directed onto the cold (10–20 K) sample holder, and the samples were condensed over some minutes.

The thermodynamic equilibrium conditions are not fulfilled for such a kind of sample preparation. These samples have irregular macroscopic structure consisting of tiny crystallites and look like snow in visual observation. Therefore, these samples are referred to as ‘snowlike’ hereafter. FE emission is not observable in such a kind of sample.

3. Luminescence of solid krypton

Since FE luminescence is observed only in samples with very good quality, spectroscopic investigations of FE luminescence are experimentally rather complicated. Nevertheless, some information is published about FE luminescence in solid Kr [3, 5]. Lack of data about FE luminescence in solid Kr is partially caused by the purity of Kr gas used. Namely, commercially available Kr gas always contains a certain amount of the Xe impurity and Xe atoms in a Kr matrix are extremely good luminescence centres.

Figure 1(a) shows a typical luminescence spectrum of a good-quality Xe-free Kr sample (Xe < 5.0 ppm). Broad-band luminescence in the region of 8.6 eV is assigned to the STE emission and a narrow peak at $E_{\text{ex}} = 10.14$ eV is due to the radiative decay of the FE. On the low-energy side of the FE, a phonon satellite is located. A small structure on the high-energy side of the FE is an experimental artefact caused by the detection system. In the present work, luminescence spectra of practically Xe-free solid Kr were observed for the first time.

Figure 1(b) demonstrates a typical luminescence spectrum of solid Kr with some Xe impurity. This sample was also grown from gas phase near thermodynamic equilibrium conditions. The spectrum is more complicated due to the Xe impurity, which causes clearly observable emission bands at 9.65 and 9.69 eV. The bands in the region from 6.7 to 8.4 eV, which overlap with the STE band of Kr, originate partly from (KrXe)* as well as Xe₂* molecular centres. (An) additional Xe-connected sub-band(s) also exist(s) in the region 8.5–8.8 eV.

4. STE luminescence of solid krypton

The STE luminescence of solid Kr has been studied several times by various groups using different kinds of excitation [5–7]. Nevertheless, the maxima and widths of the STE emission band reported in the literature vary significantly (see table 1). Mainly two factors induce such large variations—the amount of Xe impurity and the quality of the sample, i.e. existence of a macroscopic crystal structure.

The Xe impurity causes the appearance of new Xe-connected emission bands and some of them overlap with the STE luminescence band, complicating the analysis (see figure 1). As a result, the experimentally detected luminescence band shifts to the high-energy side and its shape also changes.

The crystal defects induce a red-shift of the STE luminescence band. Savchenko *et al* [7,8] investigated the red-shift of the luminescence band during irradiation of the sample. They assumed that the STE band is the sum of two Gaussian sub-bands, the STE at a perfect crystal site and the STE associated with a defect. According to Savchenko *et al*, the red-shift during irradiation results from radiation-induced defect formation leading to an increase of the respective sub-band.

In the present work, two different kinds of sample were prepared, (i) snowlike samples and (ii) samples with good crystalline quality. In both cases, Kr gas with a negligible amount of Xe impurities was used. The STE luminescence for these samples was measured under similar conditions (see figure 2). In the snowlike sample, the STE luminescence band can be represented with a single, rather broad Gaussian (FWHM 400 meV and maximum

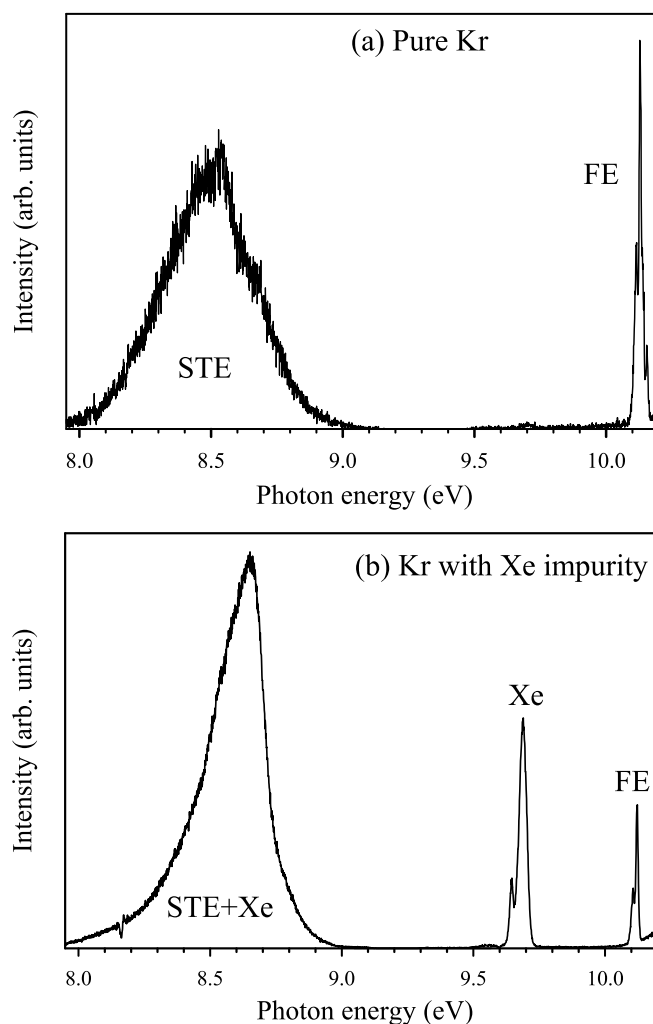


Figure 1. (a) Typical luminescence spectrum of good quality Xe-free Kr sample (purity of the gas 99.999%, <5 ppm Xe). (b) Typical luminescence spectrum of solid Kr with Xe impurity. Both spectra were measured with resolution $\Delta\lambda = 1.1 \text{ \AA}$ and excited by 10.42 eV photons (resolution $\Delta\lambda = 3.5 \text{ \AA}$) at 6 K. Convolution of the STE and Xe-connected sub-bands is marked with STE+Xe.

at 8.37 eV). The STE in a snowlike sample can occupy sites with different microscopic neighbourhoods. The broad Gaussian-shaped luminescence band is ascribed to sites with different local geometries. It is also important to point out that in the case of snowlike samples the term 'self-trapped exciton' has to be taken with reservations since trapping takes place near defects.

The luminescence band of a good-quality sample mainly arises from STEs occupying regular sites. However, the structure of a real crystal is never perfect. Therefore the luminescence band of a good-quality sample includes also some contribution from the STEs near defects. Taking into account the maximum and the width of the luminescence band from a snowlike sample, it is possible to separate the small defect-related part from the 'regular' STE band by a fitting procedure ($\sim 10\%$ from the total intensity of the curves shown in figure 2).

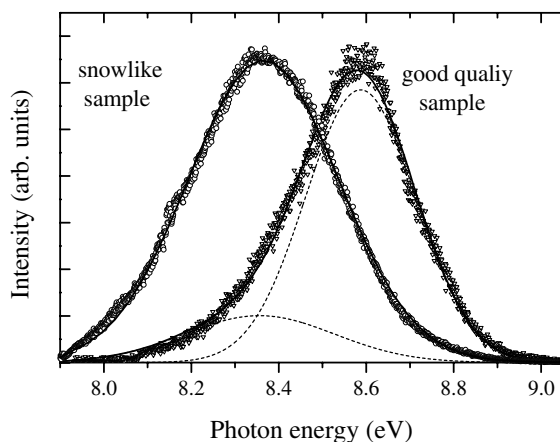


Figure 2. STE luminescence spectra for a snowlike sample and a good-quality sample, excited by 10.42 eV photons. A decomposition into two Gaussians is also shown for the good-quality sample.

Table 1. A collection of experimental data for STE luminescence band of solid Kr.

Reference	Comments	Position (eV)	FWHM (meV)	Excitation ^a
Present work	Good-quality sample	8.58 ^c	300 ^c	$h\nu = 10.42$ eV
Varding ^b [5]	STE band (fit)	8.55	200	$h\nu = 10.42$ eV
Savchenko <i>et al</i> [7]	'Pure' STE band (fit)	8.6	280	$E_e = 1$ keV
Kink <i>et al</i> [6]	Mono-crystal sample	8.5	530	x-ray
Present work	Snowlike sample	8.37 ^c	400 ^c	$h\nu = 10.42$ eV
Savchenko <i>et al</i> [7]	'Defect' STE band (fit)	8.38	370	$E_e = 1$ keV
Fugol' <i>et al</i> [8]	Snowlike sample	8.34	470	$E_e = 0.5$ keV

^a $h\nu$ means the photon energy and E_e is the energy of the electron beam.

^b Varding used Kr with a significant amount of Xe impurity.

^c Errors are estimated to be <20 meV.

As a result, the position of the maximum (8.58 eV) and the width (FWHM 300 meV) of the STE band in a regular lattice (excited by 10.42 eV photons) were determined with higher precision. The errors of the fitting results (for both peak positions and widths) were estimated to be <20 meV. Unfortunately, the error bars obtained in earlier studies are missing from the literature and therefore cannot be compared with our value.

It is directly demonstrated that the STE luminescence band near defects is shifted ~ 0.25 eV to the lower-energy side and it is also broader than the emission band of STEs in the regular lattice (see figure 2). Due to the high-purity Kr, the results from the present work do not suffer from the disturbances induced by Xe impurity. However, it is important not to overestimate the implications of the new values given in table 1, since properties of RGS are known to be sample sensitive. Additionally, the position and width of the STE luminescence band depend in some degree on the type of excitation. The very small width for the STE band as observed by Varding [5] appears to be influenced by the overlap of the Xe impurity emission (see figure 1(b)) and should therefore be excluded.

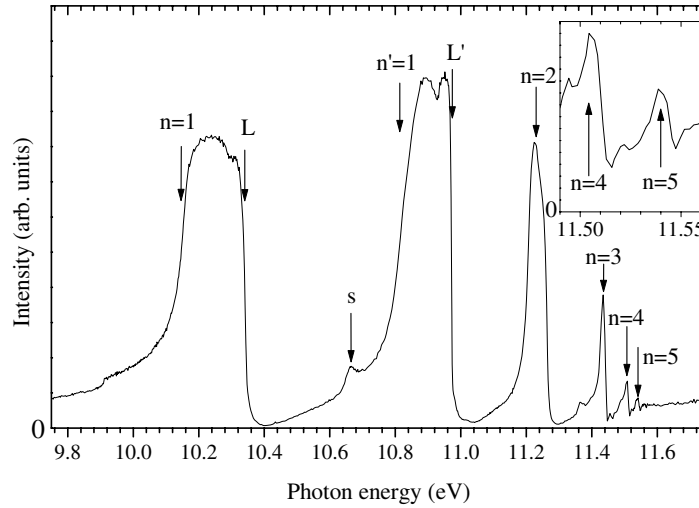


Figure 3. High-resolution reflection spectrum of solid Kr ($T = 6$ K), measured with resolution $\Delta\lambda = 0.6$ Å. The inset shows $n = 4$ and 5 excitons in an enlarged scale. The $n = 5$ exciton was observed for the first time.

5. Reflection spectra

Reflection spectra of solid Kr have been measured several times in the past (see e.g. [1, 9]). The structure of the sample and particularly of its surface, surface contamination etc can seriously influence reflectivity. In the present work, the quality of the samples and also vacuum conditions were considerably improved. New data permit us to determine more accurately values of exciton characteristics in solid krypton. Also some new aspects of the ‘intermediate-exciton’ model will be discussed on the basis of the new high-resolution reflection data.

In solid Kr, it is generally accepted that the excitons with main quantum number $n \geq 2$ are Wannier-type excitons, i.e. the electron and hole are spatially well separated. The energies of Wannier excitons are given by [2]

$$E_n = E_g - B^* \frac{1}{n^2} \quad \text{and} \quad B^* = \frac{\mu e^4}{8\varepsilon_r^2 \varepsilon_0^2 h^2}. \quad (1)$$

Here, E_g is the bandgap energy, B^* is the binding energy of the exciton series, n is the main quantum number, $\mu = m_e m_h / (m_e + m_h)$ is the reduced mass of the exciton, m_e and m_h are the effective masses of the electron and hole, ε_0 is the vacuum permittivity, ε_r is the relative dielectric constant of the medium, h is the Planck constant and e is the elementary charge. Analogous to the hydrogen atom, the so-called exciton radii are defined as

$$r_n = \frac{h^2 \varepsilon_r \varepsilon_0}{\pi \mu e^2} n^2. \quad (2)$$

The Wannier–Mott model is a good approximation for exciton radii $r_n \gg$ lattice constant.

As mentioned before, the valence band of solid Kr is split into two sub-bands due to the spin–orbit interaction, and therefore two exciton series exist. Figure 3 presents a high-resolution ($\Delta\lambda = 0.6$ Å) reflection spectrum of the excitonic region in solid Kr up to the bandgap energy $E_g = 11.59$ eV. The members of the $\Gamma(\frac{3}{2})$ exciton series are marked with $n = 1, 2, 3, 4, 5$ and the first member of the $\Gamma(\frac{1}{2})$ series with $n' = 1$. The well pronounced $n = 5$ member of the Wannier series is observed for the first time. The surface exciton is designated s .

Table 2. A collection of the experimental values of exciton energies in solid krypton.

Reference		Baldini [1]	Saile [9]	Present work ^a
Experimental method		absorption	absorption	reflection
Temperature		20 K		6 K
Volume $\Gamma(\frac{3}{2})$	$n = 1$	10.19	10.17	10.137 ^b
	$n = 2$	11.24	11.23	11.23
	$n = 3$	11.48	11.44	11.43
	$n = 4$	—	11.52	11.50
	$n = 5$	—	—	11.54
Volume $\Gamma(\frac{1}{2})$	$n' = 1$	10.88	10.86	— ^c
	$n' = 2$	11.95	11.92	11.90
	$n' = 3$	—	(12.21)	12.15
Surface $\Gamma(\frac{3}{2})$	$n = 1^d$	—	9.95	9.94
	$n = 1^d$	—	10.02	—
	$n = 2$	—	11.03	—
Surface $\Gamma(\frac{1}{2})$	$n' = 1$	—	10.68	10.66

^a Mean values averaged over three measurements. Error is estimated to be <10 meV.

^b A value from high-resolution luminescence measurements [5]. Error is estimated to be <2 meV.

^c This exciton is observed, but due to the longitudinal–transverse splitting the exact position is not well defined.

^d Splitting due to the crystal field.

In contrast to the sharp maxima of $n \geq 2$ excitons, the reflection peaks of the $n = 1$ and $n' = 1$ excitons are significantly broadened. This originates from the well known exciton–polariton nature of these excitons, discussed in detail by Kink and Selg [10]. The comparatively large widths are due to the longitudinal–transverse splitting of the exciton–polaritons. The determination of the energies of the transverse and longitudinal excitons from reflectivity spectra requires a detailed analysis of the experimental curves in terms of theory, as was demonstrated for solid Xe [10]. Such an analysis was not carried out in this work because only the energy of the transverse $n = 1$ exciton is required for the following discussion. This energy was taken from high-resolution luminescence measurements [5]. It corresponds to the maximum of the FE line. In figure 3, the respective value is indicated by an arrow. The arrows indicating the energetic positions of the transverse $n' = 1$ and the longitudinal $n = 1$ (L) and $n' = 1$ (L') excitons are only estimates.

The positions of the well defined reflection peaks ($n \geq 2$) are collected in table 2 (mean values averaged over three measurements). The error of the mean values of the present work is estimated to be <10 meV. The numerical value for the $n = 1$ exciton is the peak energy taken from FE luminescence (transverse exciton), with an experimental uncertainty estimated to be <2 meV [5].

In figure 4, the energetic positions of the $\Gamma(\frac{3}{2})$ excitons are plotted as a function of $1/n^2$. Obviously, the energetic positions of all members can be described with high accuracy by equation (1), the so-called ‘Wannier formula’. The full line in figure 4 is the result of a linear regression. It permits us to determine the bandgap energy E_g (11.59 ± 0.01 eV) and the binding energy B^* (1.45 ± 0.02 eV) of the Wannier series. From these results, the reduced mass of the exciton, μ , can be calculated. Using $\epsilon_r = 1.88$ [13], $\mu = (0.377 \pm 0.005)m_0$ (m_0 : free electron mass) is obtained.

For comparison purposes, in table 2 the respective experimental values given by Baldini [1] and Saile [9] are included. There is good agreement for the energy positions of $n \geq 2$ excitons as far as they were measured by the authors. Concerning the energy of the $n = 1$ exciton, however,

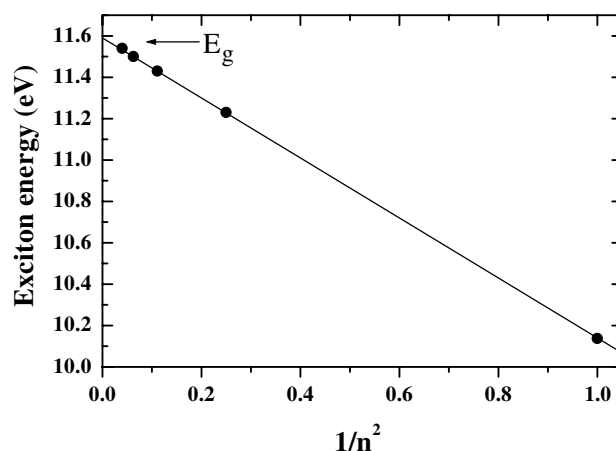


Figure 4. Exciton energies (mean values) of the $\Gamma(\frac{3}{2})$ series as a function of $1/n^2$. A linear regression and bandgap energy are shown as well.

the literature values are considerably higher than the result from high-resolution luminescence measurements. This disagreement is interesting because the higher values reported in the past could not be described by the Wannier formula. Because of the systematic deviations of the energies of the $n = 1$ excitons in RGSs from the Wannier formula, the $n = 1$ excitons were generally classified as ‘intermediate’ excitons. A detailed discussion of the nature of $n = 1$ excitons in RGSs is included in [9, 11]. Different theoretical approaches have been developed to explain the systematic deviations. According to our results, such a deviation does not exist in the case of solid Kr. The same is true for solid Xe [12].

The discrepancy between our results and the literature results is explained in the following way. For the deduction of the energy values, the authors did not evaluate their data taking into account the exciton–polariton model in a quantitative manner, like, for example, Kink and Selg [10]. Although the longitudinal–transverse splitting had already been reported in [9] for all RGSs, the respective values were obviously estimates from energetic positions of maxima in reflection/absorption. The reference given in [9] does not include details. Since high-resolution FE luminescence spectra are now available, the former kind of determination of $n = 1$ exciton energies is obsolete. Moreover, the additional member of the exciton series ($n = 5$) observed allows for a more accurate determination of the bandgap energy and the binding energy of the exciton series.

The deviations of $n = 1$ exciton energies from the Wannier formula were ascribed to the small exciton radii. Indeed, for solid Kr, from the Wannier model a radius 2.64 Å for $n = 1$ excitons is obtained, which has to be compared with the nearest-neighbour distance 3.98 Å. Therefore, it is not allowable to conclude that our results rule out the concept of ‘intermediate’ excitons for solid Kr. As is shown in [9], the concept of ‘intermediate’ excitons includes corrections to the Wannier energy with different signs. It is entirely reasonable that these contributions more or less cancel out in the case of solid Kr.

In this context we would like to point out that for solid Ar and solid Ne the deviation from the Wannier values is so large that a more accurate determination of the transverse–longitudinal splitting of $n = 1$ exciton energies will not remove the deviation from the Wannier model. In other words, at least in the light RGSs, the model of an ‘intermediate exciton’ is definitely needed to interpret the experimental results.

Table 3. Comparison of the parameters for exciton series in solid Kr.

	Baldini [1] ^a	Saile [9] ^b	Present work ^b
Binding energy B^* (eV)	1.73	1.53	1.45 ± 0.02
Bandgap energy E_g (eV)	11.67	11.61	11.59 ± 0.01
Reduced mass μ (m_0)	0.41	0.40	0.377 ± 0.005

^a Baldini used the value $\varepsilon_r = 1.80$.

^b The value $\varepsilon_r = 1.88$ was used.

As we observed more members of the exciton series of solid Kr than ever before, the deduction of exciton parameters such as the binding energy and the reduced mass are more reliable than the values from the literature. Respective numerical values are collected in table 3. The error bars for the deduced quantities were estimated on the basis of the least-squares method.

It would be highly desirable to deduce information concerning the individual effective masses of the electron and the hole (m_e and m_h) from the reduced exciton mass μ . This is by no means trivial, because one of the unknown masses should be known from another measurement. Moreover, two additional complications exist. First, it is expected that the effective hole mass is anisotropic, leading to an anisotropic reduced exciton mass [14]. Second, it is predicted that there exist two different kinds of hole: light and heavy [15]. However, notwithstanding theoretical considerations, such effects are not observable either in reflection or luminescence spectra. Therefore, in the simplest approximation, the anisotropy may be ignored, interpreting the values for m_h and μ as mean values.

No experimental values for the effective electron mass *near the bottom* of the conduction band have been determined. Bader *et al* [16] reported an experimental value $m_e = 1.1m_0$, found on the basis of low-energy electron transmission data. Unfortunately, this method only gives a value for higher conduction-band states. A theoretical value for m_e , $m_e = 0.42m_0$, was introduced by Rössler [17]. It is in good agreement with calculations by Kunz and Mickish ($m_e = 0.418m_0$) [15]. Taking $m_e = 0.42m_0$ and $\mu = 0.377m_0$, we obtain $m_h = 3.65m_0$.

6. Conclusions

In the present work, the luminescence spectrum of a practically Xe-free good-quality solid Kr sample was measured for the first time. The influence of the sample crystal structure and Xe impurity on the shape and on the location of the STE band was investigated. It was directly demonstrated that the defects in the crystal induce a red-shift of the STE luminescence band. Besides luminescence measurements, new high-resolution reflection measurements were performed. On the basis of high-resolution reflection measurements, more accurate values of several parameters concerning excitons in solid Kr (reduced mass of the exciton, binding energy of the exciton series etc) were determined. It is important to note that series of good-quality and snowlike samples were prepared and investigated, demonstrating a good reproducibility of the main experimental results.

Acknowledgments

This work was supported by the Deutsche Forschungsgemeinschaft (project DFG-Zi 159/2) and Bundesministerium für Bildung und Forschung (grant 05 ST8GUI 6). VK also gratefully acknowledges support of the EC FW5 ‘Centres of excellence’ programme (project ICA1-1999-70086) and the Estonian Science Foundation (grant 4508).

References

- [1] Baldini G 1962 *Phys. Rev.* **128** 1562
- [2] Zimmerer G 1987 *Excited State Spectroscopy in Solids* ed U M Grassano and N Terzi (Amsterdam: North-Holland) p 37
- [3] Varding D, Becker J, Frankenstein L, Peters B, Runne M, Schröder A and Zimmerer G 1993 *Low Temp. Phys.* **19** 427
- [4] Zimmerer G 1991 *Nucl. Instrum. Methods Phys. Res. A* **308** 178
- [5] Varding D 1984 *PhD Thesis* The University of Hamburg
- [6] Kink M, Kink R, Kisand V, Maksimov J and Selg M 1997 *Nucl. Instrum. Methods Phys. Res. B* **122** 668
- [7] Savchenko E V, Ogurtsov A N, Grigorashchenko O N and Gubin S A 1994 *Chem. Phys.* **189** 415
- [8] Fugol' I Ya, Savchenko E V, Ogurtsov A N and Grigorashchenko O N 1993 *Physica B* **190** 347
- [9] Saile V 1980 *Appl. Opt.* **19** 4115
- [10] Kink R and Selg M 1979 *Phys. Status Solidi b* **96** 101
- [11] Schwentner N, Koch E-E and Jortner J 1985 *Electronic Excitations in Condensed Rare Gases (Springer Tracts in Modern Physics vol 107)* (Berlin: Springer)
- [12] Zimmerer G 1998 *J. Low Temp. Phys.* **111** 629
- [13] Fugol' I Ya 1978 *Adv. Phys.* **27** 1
- [14] Ratner A M 1996 *Phys. Rep.* **269** 197
- [15] Kunz A B and Mickish D J 1973 *Phys. Rev. B* **8** 779
- [16] Bader G, Perluzzo G, Caron L G and Sanche L 1984 *Phys. Rev. B* **30** 78
- [17] Rössler U 1970 *Phys. Status Solidi* **42** 345